Acta Chemica Scandinavica, 1995: 49: 96–102
Printed in Belgium – all rights reserved

ACTA
CHEMICA SCANDINAVICA
ISSN 0904–213X

The Solubility of SnO_2 in $NaF–AlF_3–Al_2O_3$ Melts

Haiming Xiao, Jomar Thonstad† and Sverre Rolseth

Department of Electrochemistry, Norwegian Institute of Technology, N-7034 Trondheim, Norway

Xiao, H., Thonstad, J. and Rolseth, S., 1995. The Solubility of SnO_2 in $NaF–AlF_3–Al_2O_3$ Melts. – Acta Chem. Scand. 49: 96–102 © Acta Chemica Scandinavica 1995.

$NaF–AlF_3–Al_2O_3$ melts were saturated with SnO_2 and analyzed for tin by X-ray fluorescence. The solubility of SnO_2 increased with decreasing Al_2O_3 concentration and increased with increasing temperature, and it showed a maximum at a NaF/AlF_3 molar ratio (CR) of 3. Model fitting showed that the most likely dissolved species was $SnO_2AlF_6^{3-}$, and below ca. 1 wt% Al_2O_3 the oxyfluorides $SnOF_4^{2-}$ and $Sn_2O_2F_8^{4-}$ were predominant. It was also found that the solubility of SnO_2 increased with decreasing oxygen partial pressure over the melts, indicating the formation of divalent tin species.

In the electrolytic production of aluminium the electrolyte is composed of a molten mixture of $NaF–AlF_3$-CaF_2 in which the raw material Al_2O_3 is dissolved. The composition of the fluoride solvent is not far from that of cryolite (Na_3AlF_6), because this compound exhibits a very high solubility of alumina, i.e. 12–14%[1] (concentrations are given in weight %).

As a consequence of the high solubility for alumina other oxides also exhibit a certain solubility in cryolite melts, which can be represented by exchange reactions of the type

$$M_xO_y + (2y/3)\,Na_3AlF_6 = (y/3)\,Al_2O_3 + xMF_{2y/x} + 2yNaF$$

In most cases this reaction is shifted to the left, but nevertheless solubilities of various oxides in the range of 0.5–2% are not uncommon.[2,3]

Solubility data for oxides in cryolite melts were first reported by Belyaev *et al.*[2] and by Rolin and Bernard.[3] More extensive studies of freezing-point depression by addition of oxides to cryolite, of phase diagrams and solubilities as a function of fluoride composition have since been reported for a number of systems including TiO_2, Cr_2O_3, ZnO, Cu_2O, ZrO_2, NiO, FeO, Fe_2O_3, CeO_2 and La_2O_3.[4–12]

The solubility of oxides in these melts is of particular interest for attempts to develop 'inert' oxygen-evolving anodes for aluminium production to replace the present consumable carbon anode. 'Inert' electrode materials consist of ceramic oxides or possibly metals coated with an oxide layer. The primary requirements for such anode materials are good electronic conductivity and low solubility in the cryolite melt. One candidate material which has received much attention is tin oxide, SnO_2.

In the present work a study of the solubility of SnO_2 in $NaF–AlF_3–Al_2O_3$ melts was undertaken. The solubility of SnO_2 was determined for varying Al_2O_3 concentrations and NaF/AlF_3 molar ratios (CR), and as a function of temperature. Attention was also paid to the effect of oxygen partial pressure on the solubility of SnO_2.

Experimental

To determine the solubility of tin oxide, pellets made of pure SnO_2 powder (Merck) were equilibrated with the melts. The melts were prepared from handpicked Greenland cryolite, sublimed AlF_3, reagent-grade NaF and technical-grade Al_2O_3. The oxide content of the Greenland cryolite was determined on a LECO instrument[13] (carbothermic reduction) to correspond to a content of ca. 0.2% Al_2O_3, which was used as a correction to the alumina concentration based on the weighed-in amount of alumina.

A sketch of the experimental apparatus is shown in Fig. 1. A platinum crucible containing the melt and the SnO_2 pellets was placed in a furnace. The temperature of the melt was measured directly with a standardized Pt–Pt10%Rh thermocouple protected by a platinum tube which was immersed in the melt. The temperature gradient inside the furnace was measured, and a good isothermal zone was attained. A mechanical stirrer made of nickel was used to agitate the melt. In most experiments an argon or argon–air atmosphere was maintained in the furnace, but also oxygen and CO_2–CO mixtures were used.

Samples of the melt were siphoned by dipping a quartz tube into the melt. The analysis of the samples with

† To whom correspondence should be addressed.

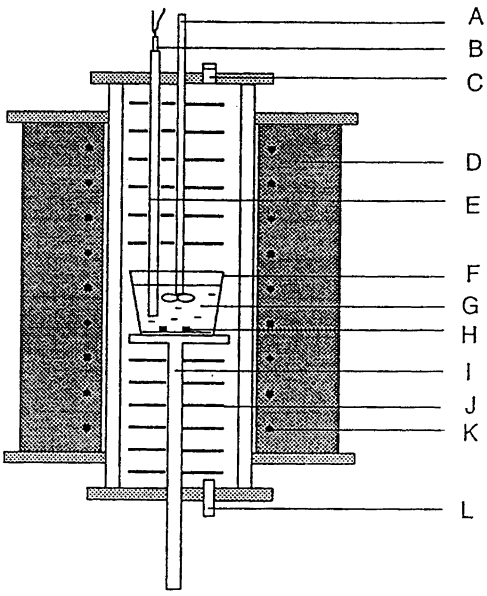

Fig. 1. Sketch of the experimental apparatus for determining solubility: (A) stirrer, (B) thermocouple, (C) hole for sampling, (D) insulation, (E) platinum tube, (F) platinum crucible, (G) melt, (H) SnO_2 pellets, (I) sintered alumina supporter, (J) radiation shields, (K) heating element, (L) gas inlet.

respect to tin was carried out by X-ray fluorescence. Some standard samples were prepared to calibrate the analytical method. It was assessed that the sensitivity and the limits of error of the analytical method were 0.001 wt% and ± 0.002 wt%, respectively, for the analysis of the content of SnO_2 in the samples.

In order to determine the equilibration time, the duration of the measurements was varied, and a plot of the SnO_2 content of the melt versus time for dissolution is shown in Fig. 2. It indicates that the equilibration time was ca. 2.5 h. There did not seem to be any significant difference in the results for samples taken after 3 h and after 5 h, so the duration of the experiments was fixed at 3.5 h.

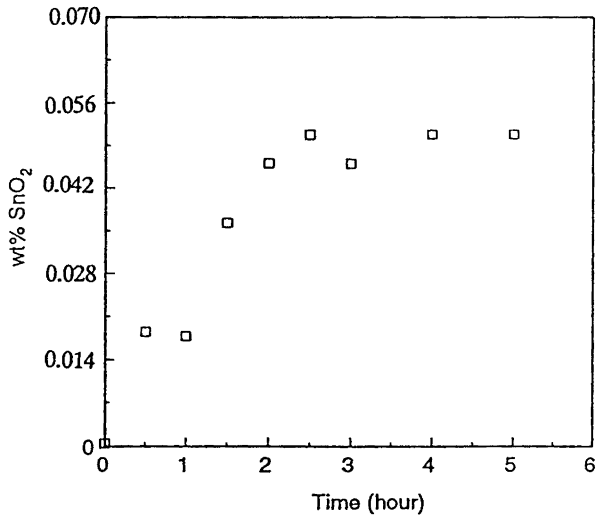

Fig. 2. Experimental results illustrating the time needed for equilibration of SnO_2 with the melt. SnO_2 in pure cryolite, 1040 ± 2 °C.

Results and discussion

Effect of the alumina concentration. Results for the solubility of SnO_2 in cryolite melts with varying alumina concentration are presented in Fig. 3, where the curve was obtained by regressive analysis of the experimental points. These data were obtained at 1045 ± 5 °C by passing oxygen gas through the furnace (Fig. 1). The reason for maintaining an oxygen atmosphere was to ensure that the dissolved SnO_2 remained in the tetravalent state, as it was relevant to determine the solubility under oxidizing conditions. However, tests performed in inert atmosphere (Ar) gave identical results.

As shown in Fig. 3, the solubility of tin oxide increased markedly with decreasing alumina concentration, especially for concentrations below 1%. Data due to Belyaev *et al.*[2] and to Rolin and Bernard[3] are also plotted in Fig. 3. These data appear to be lower at 5% Al_2O_3[2] and in pure cryolite,[3] but this is because of the lower temperatures used (1000 and 1030 °C). If the temperature coefficient obtained in the present work (Table 1) is taken into account, the agreement with the present data is fair.

The scatter of the measured solubility data is rather large. This can be due to the relatively low solubility of tin oxide, giving rise to experimental and analytical errors

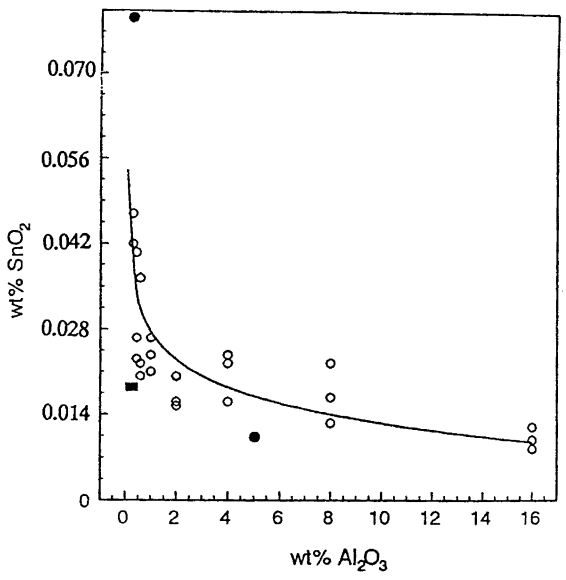

Fig. 3. Solubility of SnO_2 in cryolite–alumina melts as a function of the alumina concentration: ○, present work (1045 ± 5 °C); ●, Belyaev *et al.* (1000 °C);[2] ■, Rolin and Bernard (1030 ± 15 °C).[3]

Table 1. Solubilities of SnO_2 at different temperatures in a melt with CR = 2.2, 5% CaF_2, 5% Al_2O_3.

T/°C	SnO_2 (wt%)
950	0.008
865	0.009
975	0.013
1000	0.019
1025	0.023
1050	0.023
1075	0.027

in the measurements. Owing to an error in the standards used initially for XRF analysis, previously published solubility data[14,15] are too high by a factor of 1.43.

Effects of CR and LiF. Figures 4 and 5 show the solubility of SnO_2 in pure $NaF–AlF_3$ and in $NaF–AlF_3–Al_2O_3$(sat) melts respectively, as a function of CR. These data were obtained in an argon atmosphere. To minimize evaporation of the melt, the platinum crucible was housed inside an alumina crucible sealed with an alumina lid. For sampling the lid was removed by means of a molybdenum wire attached to it.

From the two figures one can see that the CR has a marked effect on the solubility, and maximum solubility occurs at around CR = 3.0 in both cases. The solubility of SnO_2 in a melt with a high content of LiF (CR = 3, 5 wt% Al_2O_3, 8 wt% LiF) was also determined and found to be very low (i.e. 0.005 wt%).

Effect of temperature. A low melting composition (CR = 2.2, 5 wt% CaF_2, 5 wt% Al_2O_3) was selected to study the effect of temperature. The liquidus temperature of this melt is 946°C,[16] and the temperature was varied in the range 950–1075°C. The results, which are presented in Table 1, show that the solubility of SnO_2 in the melt increased substantially with increasing temperature.

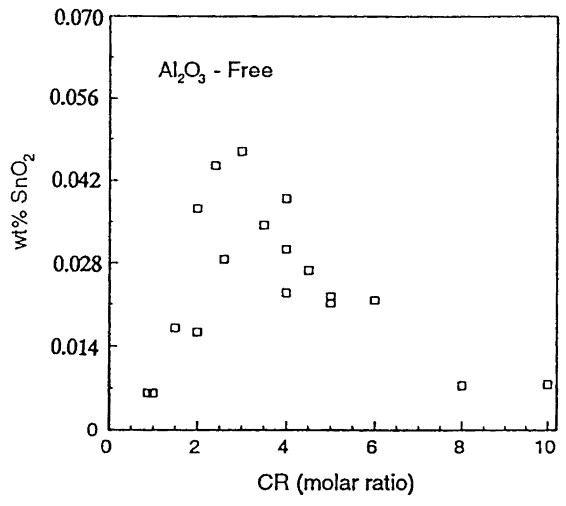

Fig. 4. Solubilities of SnO_2 in $NaF–AlF_3$ melts with different NaF/AlF_3 molar ratios (CR). 1020±2°C.

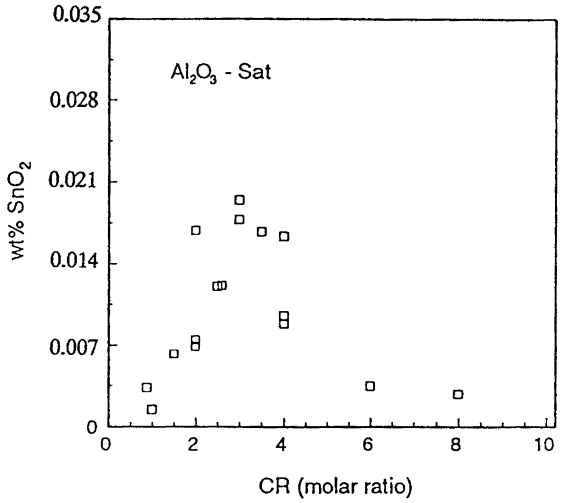

Fig. 5. Solubilities of SnO_2 in $NaF–AlF_3–Al_2O_3$ (sat) melts with different NaF/AlF_3 molar ratios (CR). 1000±2°C.

The partial enthalpy of solution ($\Delta\bar{H}_{SnO_2}$) of SnO_2 in the melt can be obtained from the solubility data. At saturation we have

$$SnO_2(s) = SnO_2(diss) \tag{1}$$

$$\Delta G^\circ = -RT \ln \frac{a_{SnO_2(diss)}}{a_{SnO_2(s)}} \tag{2}$$

where the activity of the solid SnO_2 ($a_{SnO_2(s)}$) is equal to unity. Since the solubility is low, we can assume Henrian behaviour:

$$a_{SnO_2(diss)} = kx_{SnO_2(diss)} \tag{3}$$

where k is the activity coefficient and x is the concentration, in this case in wt%.

By introducing the Gibbs–Helmholtz equation, we obtain the following equation

$$\frac{\partial(\ln x_{SnO_2(diss)})}{\partial(1/T)} = -\frac{\Delta\bar{H}_{SnO_2}}{R} \tag{4}$$

Therefore a plot of ln(wt% SnO_2) vs. $1/T$ should be linear, provided that the assumption of Henrian behaviour holds and ΔH_{SnO_2} is independent of temperature. In Fig. 6 the solubility data for SnO_2 are plotted in this manner, showing a good correlation. The least-squares equation is

$$\ln(\text{wt\% } SnO_2) = 8.287 - 15466.3/T \tag{5}$$

The partial molar enthalpy for dissolution of the oxide, $\Delta\bar{H}_{SnO_2}$, was calculated to be 129 kJ mol^{-1}. De Young[9] reported that the partial molar enthalpies of dissolution of Fe_2O_3 and NiO in $NaF–AlF_3–Al_2O_3$ melts are 138 and 186 kJ mol^{-1}, respectively, which are of similar magnitude as the present value for SnO_2.

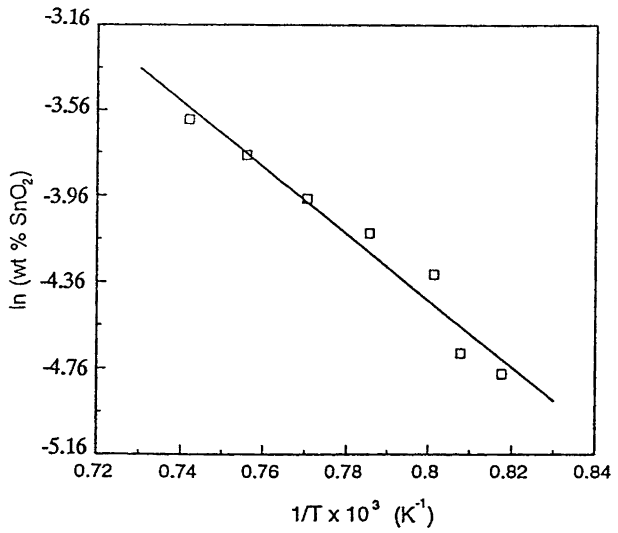

Fig. 6. The natural logarithm of the saturation concentration of dissolved SnO_2 as a function of the reciprocal temperature (950–1075 °C) in a melt with the composition CR = 2.2, 5% CaF_2, 5% Al_2O_3.

Mechanism of SnO_2 dissolution and model fitting. As a first attempt to elucidate the nature of the dissolved species for the dissolution of SnO_2 in cryolite-based melts, the following reaction can be considered:

$$SnO_2(s) + (4/3)AlF_3 = SnF_4(diss) + (2/3)Al_2O_3 \quad (6)$$

$\Delta G^\circ_{1000\,^\circ C} = 115$ kJ mol^{-1} (Refs. 17 and 18)

with the equilibrium constant

$$K_6 = \frac{a_{SnF_4}\, a_{Al_2O_3}{}^{2/3}}{a_{AlF_3}{}^{4/3}} \quad (7)$$

The shape of a plot of the activity of SnF_4 (or dissolved SnO_2) as a function of the alumina concentration can be obtained from eqn. (7) by introducing data for the activities of AlF_3 and Al_2O_3 as a function of the concentration of alumina. In this calculation activity data for AlF_3 in Na_3AlF_6–Al_2O_3 melts, given by Sterten and Meland,[19–21] and the relationship between concentration and activity of Al_2O_3, given by Dewing:[22]

$$a_{Al_2O_3} = \left(\frac{x_{Al_2O_3}}{x^s_{Al_2O_3}}\right)^{2.77} \quad (8)$$

where $x^s_{Al_2O_3}$ is the saturation concentration for Al_2O_3, were used.

However, it can easily be seen that this reaction scheme is not a realistic model for the dissolution process, since it predicts a far stronger dependence on alumina concentration (several orders of magnitude) than that found experimentally (cf. Fig. 3).

The very positive ΔG° for reaction (6) and the experimental fact of low SnO_2 solubility imply that the bond between Sn and O in tin oxide is not easy to break and that tin oxide probably dissolves as some oxyfluoride species or as SnO_2 associated with, e.g., aluminium fluoride ions, such as $Sn_pO_qF_r^{y-}$ or $SnO_2Al_xF_{y+3x}^{y-}$ in the melt. The corresponding reactions can be written as follows:

$$SnO_2 + (x/p)AlF_3 + (y/p)NaF = (1/p)[Sn_pO_{(2p-3x/2)}F_{y+3x}]^{-y/p} + (x/2p)Al_2O_3 + (y/p)Na^+ \quad (9)$$

$$K_9 = \frac{a_{Sn_pO_{(2p-3x/2)}F_{(y+3x)}{}^{y-}}{}^{1/p}\, a_{Al_2O_3}{}^{x/2p}}{a_{AlF_3}{}^{x/p}\, a_{NaF}{}^{y/p}} \quad (10)$$

$$SnO_2 + x\,AlF_3 + y\,NaF = SnO_2Al_xF_{y+3x}^{y-} + y\,Na^+ \quad (11)$$

$$K_{11} = \frac{a_{SnO_2Al_xF_{y+3x}{}^{y-}}}{a_{AlF_3}{}^{x}\, a_{NaF}{}^{y}} \quad (12)$$

In these equations the activities of solid SnO_2 and Na^+ are set equal to unity, and the activity of alumina is also equal to unity when the melt is saturated with alumina. Sterten *et al.*[19–21] have given activity data for NaF and AlF_3 in melts of pure NaF–AlF_3 and alumina-saturated NaF–AlF_3 as a function of CR. According to eqns. (10) and (12) and the activity data given in the literature,[21] the concentration profiles of some tentative dissolved species as a function of the CR were calculated. The concentration profiles for $Sn_2OF_{12}^{6-}$, $SnOF_4^{2-}$, $Sn_2O_2F_8^{4-}$ and $SnO_2AlF_6^{3-}$ all showed a similar trend as the experimental data, with a maximum at around CR = 3. In general a maximum at CR = 3 is obtained for cases where $y/x = 3$.

From Fig. 3 it can be noted that there is a rather abrupt increase in the solubility of SnO_2 for alumina concentrations below 1 wt%. This may indicate that different species are formed at low and high alumina concentrations. When the solubility data are plotted on a logarithmic scale, as shown in Fig. 7, it appears that all the data might be represented by one line. However, it is also possible to draw two lines, i.e. one for low alumina concentrations (< 1%) and one for higher concentrations (> 1 wt%), although the error margin is considerable. Attempts to represent all the data by one regression line failed to give a model that fitted the experimental data, so it was reasonable to divide it into two regimes.

When only the data at low alumina concentrations (< 1 wt%) were taken into account, the slope was − 0.84, as indicated in Fig. 7. If we introduce eqn. (8), the following relationship is obtained:

$$\frac{\partial \ln(wt\%\,SnO_2)}{\partial(\ln a_{Al_2O_3})} = \frac{\partial \ln(wt\%\,SnO_2)}{2.77\,\partial(\ln x_{Al_2O_3})} \approx -\frac{0.84}{2.77} = -0.303 \quad (13)$$

which is very close to the coefficient for Al_2O_3 in the reaction

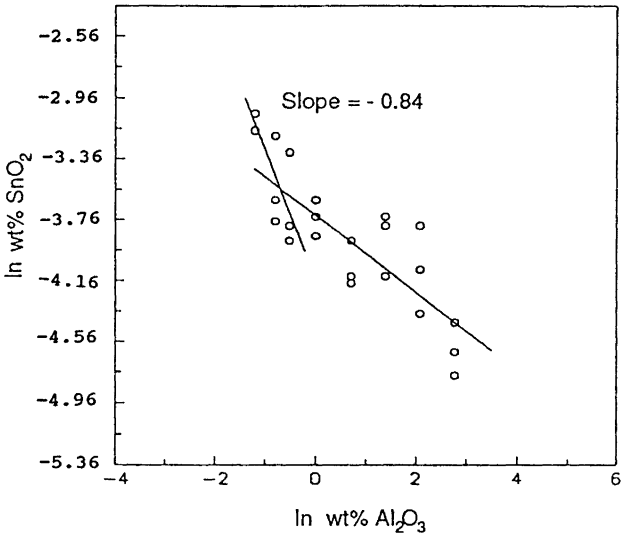

Fig. 7. The data in Fig. 3 plotted on a natural logarithmic scale.

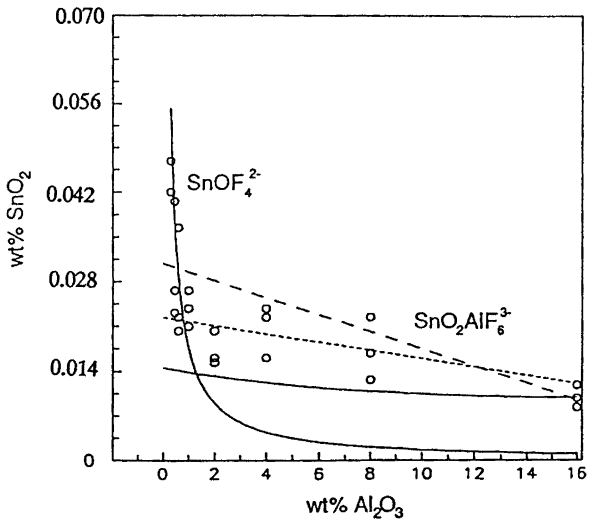

Fig. 8. Model fitting to the experimental data at varying alumina concentrations. Activity data for Al_2O_3 given by eqn. (8) and activity data for AlF_3 and NaF given by different workers were used: (——) Sterten and Meland,[19] (– – –) Kvande,[25] (- - - -) Dewing[23] and Yoshida and Dewing.[24]

$$SnO_2 + (2/3)AlF_3 + 2NaF = SnOF_4^{2-} + (1/3)Al_2O_3 + 2Na^+ \quad (14)$$

If we consider the dimer, $Sn_2O_2F_8^{4-}$, reaction (14) would be changed to

$$2SnO_2 + (4/3)AlF_3 + 4NaF = Sn_2O_2F_8^{4-} + (2/3)Al_2O_3 + 4Na^+ \quad (15)$$

The coefficient for Al_2O_3 does not agree with eqn. (13), but the scatter of the data in Fig. 7 does not exclude a steeper slope of the curve at low alumina concentrations. This problem cannot be resolved at present, so we may assume that the two species (monomer and dimer) coexist in the melt.

For higher alumina concentrations (> 1 wt%) the solubility decreased slightly with increasing alumina concentration (Fig. 3). This can be attributed to changes in the activities of NaF and AlF_3 with increasing alumina concentration for an association reaction like

$$SnO_2 + AlF_3 + 3NaF = SnO_2AlF_6^{3-} + 3Na^+ \quad (16)$$

Fig. 8 shows model fitting to the experimental data at varying alumina concentrations. One can see that the two species, $SnOF_4^{2-}$ and $SnO_2AlF_6^{3-}$, fit the data fairly well at low (<wt 1%) and at high (> 1 wt%) alumina concentrations, respectively. If $SnOF_4^{2-}$ is replaced by the dimer $Sn_2O_2F_8^{4-}$, the fit is equally good at the low alumina concentrations in question. Activity data for AlF_3 and NaF given by different workers were used. It seems that the model $SnO_2AlF_6^{3-}$ shows the best fit when the activity data given by Dewing[23] and Yoshida and Dewing[24] are used. Since Dewing and also Kvande[25] gave data only for the extremes, i.e. alumina-saturated and alumina-free melts, the fitted lines in those cases are drawn as straight lines.

Other species tested for high alumina concentrations were $SnO_2 \cdot 2AlF_6^{6-}$, but the fit did not improve, and $Sn_2OF_{12}^{6-}$, which gave a rather poor fit.

Darmois and Petit[5] carried out cryoscopic studies adding SnO_2 to cryolite, and found that the number of particles formed was three at infinite dilution, decreasing to two and one with increasing concentration. The reaction scheme according to eqn. (14) corresponds to the formation of two new particles, since (1/3) Al_2O_3 yields one particle.[1] Eqn. (15) corresponds to 1.5 particles and eqn. (16) corresponds to one new particle.

Figures 9–11 show model fitting for the species $SnOF_4^{2-}$ and $Sn_2O_2F_8^{4-}$ at varying CR values in pure NaF–AlF_3 melts and $SnO_2AlF_6^{3-}$ in alumina-saturated

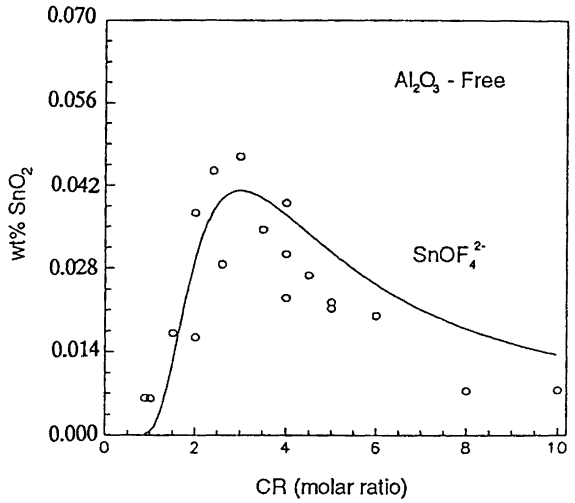

Fig. 9. Model fitting for the species $SnOF_4^{2-}$ at varying CR values in pure NaF–AlF_3 melts.

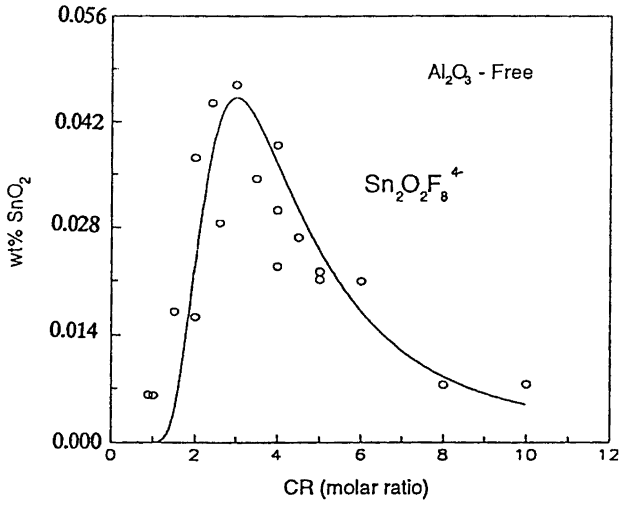

Fig. 10. Model fitting for the dimer of $SnOF_4^{2-}$, $Sn_2O_2F_8^{4-}$, at varying CR values in pure NaF–AlF_3 melts.

NaF–AlF_3 melts, respectively. Taking into account the experimental scatter, the models for Al_2O_3-free melts show reasonable agreement with the experimental data, $Sn_2O_2F_8^{4-}$ giving the best fit. For alumina-saturated melts the fit for $SnO_2 \cdot 2AlF_6^{6-}$ is also reasonable, especially at low CR values. The structure of the various SnO_2-containing species is not known, but it is likely that Sn–O–Sn and/or Sn–O–Al bridges are formed.

Effect of the oxygen partial pressure. Indications were found that the amount of tin-containing species increased under reducing conditions. Some experiments were made passing a CO_2/CO gas mixture above the melt during the solubility test. According to the standard Gibbs energy of the reaction

$$SnO_2 + 2CO = Sn + 2CO_2 \qquad (17)$$

$\Delta G^\circ_{1300\,K} = -27.681$ kJ mol^{-1} (Refs. 26 and 27)

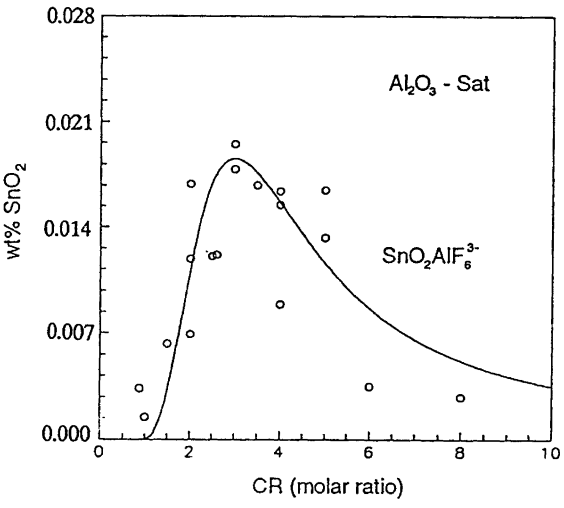

Fig. 11. Model fitting for the species $SnO_2AlF_6^{3-}$ at varying CR values in alumina-saturated NaF–AlF_3 melts.

the thermodynamic condition for the formation of metallic tin is that the ratio $CO_2/CO \leq 80/20$, and to avoid that, two standard gas mixtures with CO_2/CO ratios of 85/15 and 95/5 were chosen. The oxygen partial pressures for the two cases were calculated to be 7.40×10^{-13} and 8.52×10^{-12} atm, respectively.[26] Figure 12 shows the measured solubilities (expressed as wt% SnO_2) in cryolite–alumina melts at these two pressures, together with the curve from Fig. 3.

The solubility was much higher at low oxygen partial pressures, which may be due to the formation of divalent tin:

$$SnO_2 + CO = SnO\,(s) + CO_2 \qquad (18)$$

$\Delta G^\circ_{1300\,K} = -14.376$ kJ mol^{-1} (Refs. 26 and 27)

Pure SnO is a liquid above 1250 K,[26] and it may be soluble in the melt, forming Sn(II)-containing species. The activities of SnO at the two CO_2/CO ratios at 1300 K were calculated to be 0.67 and 0.19, respectively.

These data indicate the presence of divalent tin [Sn(II)] in the melt under these conditions. The results in Fig. 12 must only be taken as an indication of the behaviour of the system under reducing conditions, since experience has shown that it may be difficult to establish equilibrium between a molten salt and a surrounding atmosphere. A further study on this topic will be published later.

It should be pointed out that the presence of Sn(II) was highly unlikely in an argon atmosphere, since there were no reducing species in the system. The experimental fact that an oxidizing atmosphere and an inert atmosphere gave identical solubility results substantiates this claim.

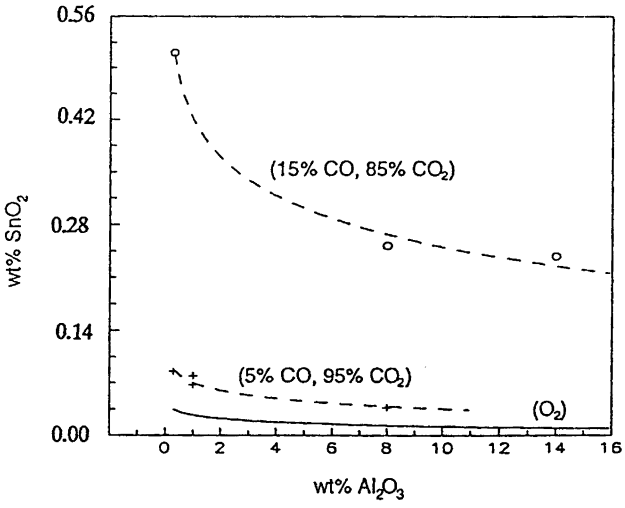

Fig. 12. Solubilities expressed as wt% SnO_2 in cryolite-alumina melts under reducing CO_2/CO atmosphere (1030±2°C). For comparison the solubility data obtained under oxygen atmosphere (Fig. 3) are included.

Implications for the use of tin oxide-based inert anodes in aluminium reduction cells. Since the problem of anode corrosion appears to be the major obstacle for the use of inert anodes in commercial aluminium reduction cells,[15,17] these solubility data have several implications regarding cell operation with tin oxide-based inert anodes.

(i) The electrolyte should have a fairly high concentration of Al_2O_3, a low CR, and the cell should be operated at low temperature to minimize the solubility of the anode material. However, when such conditions are employed, some negative effects must also be taken into account. For instance, if low melting electrolytes are chosen, the solubility of alumina is generally quite low, which may be harmful to the inert anodes.

(ii) Tin oxide is sensitive to reducing conditions. In order to keep a low corrosion rate of SnO_2-based anodes during electrolysis, any reducing conditions, including reduction by dissolved metal, should be avoided.

Acknowledgements. Financial support from the Royal Norwegian Council for Scientific and Industrial Research (NTNF) and from the Norwegian Aluminium Industry under the 'Expomat' program is gratefully acknowledged. The X-ray fluorescence analysis of tin in the samples of cryolite mixtures was carried out at the Department of Geology and Minerals, the Norwegian Institute of Technology, and a few samples were also analyzed by the Alcan Research Center, Arvida, Quebec, Canada.

References

1. Grjotheim, K., Krohn, C., Malinovsky, M., Matiasovsky,K. and Thonstad, J. *Aluminium Electrolysis, Fundamentals of the Hall-Heroult Process*, 2nd edn., Aluminium-Verlag, Dusseldorf 1982.
2. Belyaev, A. I., Rapoport, M. B.and Firsanova, L. A. *Metallurgie des Aluminiums*, VEB Verlag Chemie, Berlin 1956, 74.
3. Rolin, M. and Bernard, M. *Bull. Soc. Chim. Fr.* (1963) 1035.
4. Johansen, H. G., Sterten, Å and Thonstad, J. *Acta Chem. Scand., Ser. A 43* (1989) 417.
5. Darmois, E. and Petit, G. *C. R. Acad. Sci. (Paris), Ser. C 223* (1951) 1551.
6. Berul, S. I. and Voskresenskaya, N. K., *Russ. J. Inorg. Chem. 8* (1963) 744.
7. Belov, S. F., Gladvera, G. D., Seredina, Ivz. *Uchebn. Zav. Tsvet. Met. 23(3)* (1980) 316.
8. Hayakawa, Y. and Kido, H. *J. Electrochem. Soc. Jpn. 20* (1952) 3.
9. DeYoung, D. H. *Light Metals 1986*, Proc., The Metallurgical Soc., Warrendale, PA, 299.
10. Dewing, E. W., Haarberg, G. M., Rolseth, S., Rønne, L. and Thonstad, J. 1993. *Unpublished.*
11. Shen, S., Zhao, K. and Zhang, Y. *Rare Earth Met. 3* (1983) 1.
12. Shen, S., Zhao, K. and Zhang, Y. *Rare Earth Met. 2* (1984) 23.
13. Tarcy, G. P., Rolseth, S. and Thonstad, J. *Light Metals 1993*, The Metallurgical Soc., Warrendale, PA 1993, p. 227.
14. Xiao, H., Hovland, R., Rolseth, S. and Thonstad, J. *Light Metals 1992*, The Metallurgical Soc., Warrendale, PA 1993, p. 389.
15. Xiao, H., Thonstad, J. and Rolseth, S., in Sequeira, C. A. C. and Picard, G. S., Eds., *Electrochemical Technology of Molten Salts*, Molten Salts Forum, Vols. 1 and 2, p. 215, Trans. Tech. Publ., Switzerland 1993.
16. Rostum, Å, Solheim, A. and Sterten, Å, *Light Metals 1990*, The Metallurgical Soc., Warrendale, PA 1993, p. 317.
17. Wang, H. and Thonstad, J. *Light Metals 1989*, The Metallurgical Soc., Warrendale, PA 1989, p. 283.
18. Reed, T. B., *Free Energy of Formation of Binary Compounds. An Atlas of Charts for High Temperature Chemical Calculations*, Massachusetts Institute of Technology, Boston, MA 1971.
19. Sterten, Å and Meland, I. *Acta Chem. Scand., Ser. A 39* (1985) 241.
20. Sterten, Å. *Electrochim. Acta* (25) (1980) 1673.
21. Sterten, Å, Hamberg, K. and Meland, I. *Acta Chem. Scand., Ser. A 36* (1982) 329.
22. Dewing, E. W. *Can. Met. Quart. 13* (1974) 607.
23. Dewing, E. W. *Metall. Trans. 3* (1972) 495.
24. Yoshida, H. and Dewing, E. W. *Met. Trans. 3* (1972) 683.
25. Kvande, H. *Thermodynamics of the System NaF–AlF_3–Al_2O_3–Al*, Dissertation, University of Trondheim, NTH, Trondheim 1979.
26. Barin, I. *Thermochemical Data of Pure Substances*, VCH, Weinheim 1989, p. 1404.
27. Gurvich, L. V., Veyts, I. V. and Alcock, C. B. *Thermodynamic Properties of Individual Substances*, Vol. 2, Hemisphere Publishing Corp., New York 1990, p. 350.

Received October 22, 1994.